BBA - General Subjects 1867 (2023) 130313

Contents lists available at ScienceDirect

BBA - General Subjects

journal homepage: www.elsevier.com/locate/bbagen

Life-threatening arrhythmogenic CaM mutations disrupt CaM binding to a distinct RyR2 CaM-binding pocket

Angelos Thanassoulas [a], Vyronia Vassilakopoulou [b], Brian L. Calver [c], Luke Buntwal [c], Adrian Smith [c], Christopher Lai [c,d], Iris Kontogianni [b,e], Evangelia Livaniou [b], George Nounesis [b], F. Anthony Lai [a,c], Michail Nomikos [a,*]

[a] College of Medicine, QU Health, Qatar University, Doha, Qatar
[b] National Centre for Scientific Research "Demokritos", Agia Paraskevi, Greece
[c] Sir Geraint Evans Wales Heart Research Institute, College of Biomedical and Life Science, Cardiff University, Cardiff, UK
[d] University of Cambridge School of Medicine, Cambridge Biomedical Campus, Cambridge, UK
[e] National Technical University of Athens, Athens, Greece

ARTICLE INFO

Keywords:
Calmodulin
Ryanodine receptor
RyR2
Arrhythmias
Cardiac disease

ABSTRACT

Calmodulin (CaM) modulates the activity of several proteins that play a key role in excitation-contraction coupling (ECC). In cardiac muscle, the major binding partner of CaM is the type-2 ryanodine receptor (RyR2) and altered CaM binding contributes to defects in sarcoplasmic reticulum (SR) calcium (Ca^{2+}) release. Many genetic studies have reported a series of CaM missense mutations in patients with a history of severe arrhythmogenic cardiac disorders. In the present study, we generated four missense CaM mutants (CaM^{N98I}, CaM^{D132E}, CaM^{D134H} and CaM^{Q136P}) and we used a CaM-RyR2 co-immunoprecipitation and a [^{3}H]ryanodine binding assay to directly compare the relative RyR2-binding of wild type and mutant CaM proteins and to investigate the functional effects of these CaM mutations on RyR2 activity. Furthermore, isothermal titration calorimetry (ITC) experiments were performed to investigate and compare the interactions of the wild-type and mutant CaM proteins with various synthetic peptides located in the well-established RyR2 CaM-binding region (3584-3602aa), as well as another CaM-binding region (4255-4271aa) of human RyR2. Our data revealed that all four CaM mutants displayed dramatically reduced RyR2 interaction and defective modulation of [^{3}H]ryanodine binding to RyR2, regardless of LQTS or CPVT association. Moreover, our isothermal titration calorimetry ITC data suggest that RyR2 3584-3602aa and 4255-4271aa regions interact with significant affinity with wild-type CaM, in the presence and absence of Ca^{2+}, two regions that might contribute to a putative intra-subunit CaM-binding pocket. In contrast, screening the interaction of the four arrhythmogenic CaM mutants with two synthetic peptides that correspond to these RyR2 regions, revealed disparate binding properties and signifying differential mechanisms that contribute to reduced RyR2 association.

1. Introduction

Calmodulin (CaM) is an essential, intracellular calcium (Ca^{2+})-binding protein that controls and regulates many vital cellular processes. CaM functions as a Ca^{2+} sensor for decoding Ca^{2+} signals into downstream responses by undergoing conformational changes that promote binding to target proteins [1,2]. CaM is comprised of four Ca^{2+}-binding EF-hand motifs located in two globular N- and C-terminal domains connected by a flexible linker [3]. In cardiac muscle, CaM modulates directly or indirectly the activity of several proteins that play a key role in excitation-contraction coupling (ECC), including the cardiac ryanodine receptor type 2 (RyR2), a large homotetrameric cation channel that

Abbreviations: CaM, calmodulin; ECC, excitation-contraction coupling; RyR2, cardiac ryanodine receptor type 2; Ca^{2+}, calcium; SR, sarcoplasmic reticulum; SOICR, store-overload induced Ca^{2+} release; CPVT, catecholaminergic polymorphic ventricular tachycardia; LQTS, long QT syndrome; ITC, isothermal titration calorimetry; IP, immunoprecipitation; AEBSF, 4-(2-aminoethyl)-benzenesulfonyl fluoride; CHAPS, 3-[(3-cholamidopropyl)dimethylammonio]-1-propanesulfonate; DTT, dithiotreitol; EDTA, ethylenediaminetetraacetic acid; PIPES, piperazine-N,N′-bis(2-ethanesulfonic acid);; EGTA, ethylene glycol-bis-β-aminoethyl ether)-N, N, N′, N′-tetraacetic acid.

* Corresponding author at: College of Medicine, QU Health, Qatar University, Doha 2713, Qatar.
E-mail address: mnomikos@qu.edu.qa (M. Nomikos).

https://doi.org/10.1016/j.bbagen.2023.130313
Received 2 September 2022; Received in revised form 17 January 2023; Accepted 18 January 2023
Available online 21 January 2023

mediates Ca^{2+} release from the sarcoplasmic reticulum [4,5]. In humans, there are three CaM genes (*CALM1*, *CALM2* and *CALM3*) that are all expressed in cardiac tissue and which encode an identical protein [6]. In recent years, there have been an increasing number of genetic and clinical reports that identified a variety of CaM missense mutations in all three CaM genes, in individuals with a family history of severe cardiac disorders and early onset sudden cardiac death [7–12]. In the majority of cases, the arrhythmogenic phenotype that is driven by the missense mutations in the CaM genes is attributed either to prolonged repolarization [long QT syndrome (LQTS) phenotype] or to dysregulation of the intracellular calcium concentration in cardiomyocytes [catecholaminergic polymorphic ventricular tachycardia (CPVT) phenotype]. Interestingly, a genetic study reported five novel de novo missense mutations in *CALM2* gene, identified in three subjects presenting with LQTS (p.N98S, p.N98I, p.D134H) and 2 subjects with clinical features of both LQTS and CPVT (p.D132E and p.Q136P) [10]. While the four individuals responded to β-blocker therapy, the patient with p.Q136P mutation died suddenly during exertion despite the treatment [10]. The authors suggested that all these mutations alter conserved residues that are directly involved in the Ca^{2+} binding, causing significant reductions in Ca^{2+} binding affinity of CaM [10]. Another potential pathophysiological mechanism for these CaM mutations might involve altered CaM/RyR2 binding and thus defective regulation, as the major binding partner of CaM at the *Z*-line in cardiomyocytes is the RyR2, and reduction of CaM/RyR2 binding has been shown to result in severe cardiovascular abnormalities [13–15]. Moreover, we have previously proposed that the clinical presentation of CPVT or LQTS associated with CaM mutations may involve both altered intrinsic Ca^{2+}-binding, as well as dysregulation of RyR2-mediated Ca^{2+} release, via defective interaction of CaM with distinct region(s) of RyR2 [16–18].

In the present study, we introduced four of the aforementioned missense CaM mutations (N98I, D132E, D134H and Q136P) into human CaM sequence (Fig. 1) and we used a bacterial system to express and purify these CaM mutants as recombinant proteins. We then employed a CaM-RyR2 co-immunoprecipitation assay to directly compare the relative RyR2-binding of wild-type and mutant CaM proteins, and a [^{3}H] ryanodine binding assay to investigate the functional effects of these CaM mutations on RyR2 activity. Finally, isothermal titration calorimetry (ITC) experiments were performed to investigate and compare the interactions of the wild-type and mutant CaM proteins with various synthetic peptides located in the well-established RyR2 CaM-binding region (3581-3607aa), as well as in another putative CaM-binding region (4240-4277aa) of human RyR2.

2. Materials and methods

2.1. Plasmid construction

Human CaM clone (GenBank® accesion number AAD45181.1) in pHSIE plasmid [16,17] was subjected to site-directed mutagenesis (QuikChange II; Stratagene) to generate CaM^{N98I}, CaM^{D132E}, CaM^{D134H} and CaM^{Q136P} mutant constructs. Successful mutagenesis for all the aforementioned CaM constructs was confirmed by dideoxynucleotide sequencing (Applied Biosystems Big-Dye Version 3.1 chemistry and model 3730 automated capillary DNA sequencer by DNA Sequencing & Services™).

2.2. Protein expression and purification

CaM^{WT} and its corresponding mutants in pHSIE plasmid were expressed in *E. coli* (BL21-CodonPlus(DE3)-RILP; Stratagene) as previously described [17,18]. Briefly, after transformation, the bacterial cells were cultured at 37 °C until the A600 reached 0.6, and the protein expression was induced for 18 h at 16 °C with 0.1 mM isopropyl *β*-D-thiogalactopyranoside (IPTG; ForMedium). The induced cells were then harvested by centrifugation at 6000*g* for 10 min at 4 °C and recombinant CaM proteins were purified by one-step affinity chromatography purification [17,18]. The eluted recombinant CaM proteins following dialysis and concentration using centrifugal concentrators (Sartorius; 3000 molecular weight cut-off), were analyzed by SDS-PAGE and immunoblot analysis, which was performed as previously described [16–18]. For the immunoblot analysis, the CaM recombinant proteins were probed with an anti-CaM rabbit monoclonal antibody (1:10,000 dilution; Source Bioscience).

2.3. Preparation of cardiac heavy SR vesicles and co-immunoprecipitation assays

Heavy SR vesicles were isolated from pig cardiac muscle as previously described [17]. Pellets were resuspended to 25 mg protein/ml in homogenization buffer (10 mM Na_2PIPES pH 7.4, 0.3 mM sucrose, 0.5 mM EDTA, 0.2 mM AEBSF, 2 mM DTT and protease inhibitors) and stored at −80 °C in small aliquots. Co-immunoprecipitation assays were performed as we have previously described [16–18]. Cardiac SR microsomes (300 μg) were solubilised in 200 μL of IP buffer (20 mM Tris-

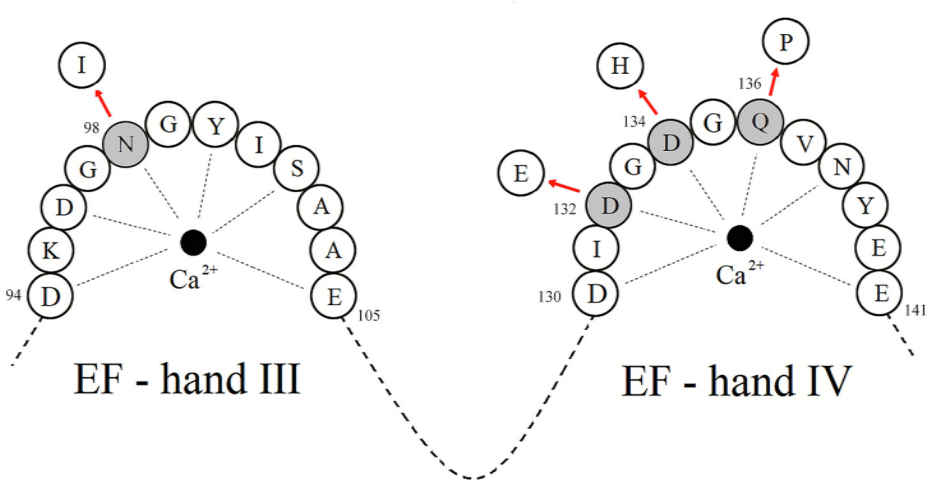

Fig. 1. Schematic representation of EF hand III and IV domains located in the C-terminal domain of CaM. Red arrows point to the amino acid substitutions responsible for the arrhythmogenic CaM mutations (N98I, D132E, D134H and Q136P) that are subject of this study. (For interpretation of the references to colour in this figure legend, the reader is referred to the web version of this article.)

HCl pH 7.4, 150 mM NaCl, 0.4% CHAPS and protease inhibitors) containing the appropriate free [Ca^{2+}] (achieved by mixing different proportions of 1 mM EGTA and 1 mM Ca^{2+} together, according to the Max Chelator software [http://maxchelator.stanford.edu/]) by overnight incubation at 4 °C with continuous mixing. The insoluble material was then pelleted at 20,000 *g* for 10 min at 4 °C, and the supernatant was removed. Concurrently, the RyR2-specific antibody, Ab^{1093} (4 μL) was captured on 20 μL nProtein-A–Sepharose beads (GE Healthcare) in 200 μL of PBS (137 mM NaCl, 2.7 mM KCl, 10 mM Na_2HPO_4, 1.8 mM KH_2PO_4, pH 7.4) overnight at 4 °C. Beads were recovered at 1500 g for 2 min at 4 °C and washed twice with the appropriate IP buffer. The solubilised SR proteins and 1 μM of CaM^{WT} or its corresponding CaM mutants were transferred into tubes with RyR2 antibody Ab^{1093}-protein-A beads, and incubated for 6 h at 4 °C with mixing. Beads were recovered at 1500 g for 2 min at 4 °C and washed twice with the appropriate IP buffer for 5 min. Immunoprecipitated proteins were then eluted with SDS-PAGE loading buffer, heated at 80 °C for 5 min, and analyzed by SDS-PAGE and western blotting using the aforementioned anti-CaM rabbit monoclonal antibody (1:5000 dilution; Source Bioscience).

2.4. [^{3}H]Ryanodine binding assays

Ryanodine binding was determined using 200 μg of cardiac SR microsomes per assay (volume 300 μL) incubated with 10 nM ryanodine containing [^{3}H]ryanodine (100 Ci/mmol, Amersham) for 90 min at 37 °C, as previously described [17,18]. The basic buffer contained 25 mM PIPES, 150 mM KCl, pH 7.1 with either 1 mM EGTA (<0.01 μM Ca^{2+}) or a series of free Ca^{2+} concentrations (values expressed as pCa 8–pCa 4 where $pCaX = -\log_{10}[Ca]X$) achieved by mixing different proportions of 1 mM EGTA and 1 mM Ca^{2+} as calculated using Max Chelator. CaM^{WT} or CaM mutants were added to a final concentration of 1 μM.

2.5. Peptide synthesis and purification

All the peptides were synthesized manually on a Rink-amide resin (loading capacity: 0.6 mmol/g) with the Fmoc strategy, following a previously described protocol [19] with slight modifications. Briefly, an excess (4 eq) of Fmoc-protected amino acids and ethyl (hydroxyimino) cyanoacetate (Oxyma) were dissolved in N,N′-dimethylformamide (DMF). The solution was left on ice for 10 min and then an excess (4 eq) of N,N′-diisopropylcarbodiimide (DIC) was added and the reaction mixture was left for another 10 min on ice and finally added to the resin for the coupling reaction (2 h). Coupling efficiency was monitored by the Kaiser ninhydrin test. After each coupling, the Fmoc group was removed from the N-terminal amino group of the resin-bound peptide with 20% piperidine in DMF. The final product was cleaved from the resin using a cocktail of trifluoroacetic acid (TFA) 93%, 1,2-ethanedithiol 2.5%, H_2O 2.5% and triisopropylsilane 2% for peptide B, while the peptides F and F scrambled, were cleaved from the resin by using the reagent R (TFA 90%, thioanisole 5%, anisole 2%, 1,2-ethanedithiol 3%) and adding an excess of Bu_4NBr (30 eq) just 5 min before the end of the cleavage treatment, in order to reduce any oxidized methionine. The crude product, obtained by precipitation with cold diethylether, was purified by semi-preparative Reverse Phase High Performance Liquid Chromatography (RP-HPLC) on a Waters system (pump 600E, detector UV-484) equipped with a 10 Nucleosil 7 C18 (250 mm × 12.7 mm, internal diameter; Macherey-Nagel) column. Elution was performed with a solvent system consisting of 0.05% TFA in water (solvent A) and 60% CH_3CN in solvent A (solvent B), by applying different gradients depending on the peptide sequence. The flow rate was 3 mL/min and the peptide peaks were detected with a UV detector at 220 nm. Analytical RP-HPLC was performed on a Waters system (pump 616E, detector 996 PDA) equipped with a LiChrospher (250 nm × 4.6 nm, internal diameter; 5 μm particle size, Merck) column, with a solvent system consisting of 0.05% TFA in water (solvent A) and 90% CH_3CN in solvent A (solvent B), by applying a linear gradient from 100% to 40% A in 23 min. The flow rate was 1 mL/min and the peptide peaks were detected with a UV detector at 220 nm. The peptides were further characterized by ESI-MS.

2.6. ESI-MS analysis

For the peptide characterization a triple quadrupole tandem mass spectrometer 310-MS TQ from Varian (Agilent Technologies; Foster City, CA, USA) was used. A sample containing approximately 0.1 mg/mL of each synthetic peptide in CH_3CN:H_2O 1:1 was directly infused to the MS/MS using a syringe pump from Harvard Apparatus (Holliston, MA) at a flow rate of 0.2 mL/min and the detection parameters were determined by operating the instrument in electrospray ionization (ESI) positive mode. (Detection parameters: detector, 1300 V; needle voltage positive, 3500 V; spray shield voltage positive, 600 V; spray chamber temperature, 55 °C; drying gas temperature 325 °C; nebulizing gas pressure 18.0 psi; drying gas pressure 19.0 psi). Instrument control, data acquisition and qualitative data analysis were performed using the MS Workstation version 6.9.3 software (Varian).

2.7. Isothermal titration calorimetry

An ITC200 (GE Healthcare) microcalorimetry system was used to study the interactions of wild type and mutant CaM proteins with the human RyR2 peptides under both Ca^{2+}-saturated and Ca^{2+}-free conditions (holo-CaM and apo-CaM, respectively). Identical purified CaM samples were dialyzed against 100 mM KCl, 10 mM HEPES (pH 7.4), 10 mM $CaCl_2$ (holo-buffer) and 100 mM KCl, 10 mM HEPES (pH 7.4), 10 mM EDTA (apo-buffer) at 4 °C. Peptides corresponding to human RyR2 CaM-recognition sites were synthesized and purified as lyophilized powder. Peptide samples for ITC experiments were dissolved directly in the appropriate dialysis buffer, to avoid buffer mismatch dilution heats. All sample solutions were thoroughly degassed before use to avoid bubble formation. In all cases, the calorimetric cell was filled with a 40 μM protein sample and the syringe was loaded with a 450 μM peptide solution. All titrations consisted of an initial 1 μL injection, followed by 14 identical 2.5 μL injections at 300 s intervals. Experiments were performed at 25 °C and a stirring speed of 1000 rpm was used to ensure a rapid equilibration of the mixture. Heat contributions from peptide dilution were accounted for in separate experiments by injecting the samples in buffer solution following identical titration protocols. These blank data are subsequently subtracted from the titration data to obtain the net binding isotherm as a function of the overall peptide concentration in the cell. All ITC data were processed using Microcal Origin software (OriginLab, Northampton, MA) equipped with calorimetric routines.

Complex formation is an equilibrium interaction that can be described by a chemical equation of the form:

$$[CaM] + [Peptide] \Leftrightarrow^{K_b} [Complex]$$

where: [*CaM*] and [*Peptide*] are the concentrations of the non-complexed CaM and peptide respectively, [*Complex*] represents the concentration of the protein-peptide complex, while $K_b = 1/K_d$ is the binding constant of the interaction.

The stoichiometry (moles of peptide bound per mol of protein) [N], the binding constant [K_b] and the binding enthalpy [Δ_rH] of the reaction are obtained, along with their corresponding uncertainties, directly from fitting the ITC experimental data to a one set-of-sites thermodynamic model. The Gibbs free energy change binding Δ_rG and the entropy change Δ_rS accompanying the complexation are calculated from the equalities:

$$\Delta_rG = RT\ ln\ K_b = \Delta_rH – T\ \Delta_rS$$

where R is the gas constant, and T is absolute temperature. The uncertainties of these parameters are estimated using error propagation

calculations.

3. Results and discussion

To investigate the impact of N98I, D132E, D134H and Q136P mutations on CaM/RyR2 binding and regulation, we initially generated the mutant CaM constructs in pHSIE plasmid vector and we used a bacterial system to express and then purify wild type and mutant CaMs as recombinant proteins, using the one-step purification protocol that we have previously successfully used and described [16–18]. Significant expression of soluble wild-type and all four mutant CaM proteins was observed. Fig. 2 shows the affinity-purified untagged recombinant CaM proteins after SDS-PAGE (left panel) and immunoblot analysis (right panel). The protein band with mobility corresponding to the predicted molecular weight (~17.4 kDa) was present for all the samples and the immunoblot analysis using an anti-CaM antibody confirmed the identity of all CaM proteins (Fig. 2).

To assess and directly compare the relative RyR2-binding affinities of CaM^{WT} and CaM mutants, we employed a co-immunoprecipitation assay, as we have previously described [16–18]. Native RyR2 from pig cardiac SR was immunoprecipitated with a purified RyR2-isoform-specific antibody in the presence of each recombinant CaM protein at two different free Ca^{2+} concentrations (0 and 100 μM) and the relative binding of CaM wild-type and mutant proteins with RyR2 was analyzed by SDS-PAGE electrophoresis and immunoblot analysis using the anti-CaM monoclonal antibody. As previously shown, endogenous CaM is not detectable on immunoblot analysis using the anti-CaM antibody, while the levels of co-immunoprecipitated RyR2 remained constant as per same porcine SR preparation analysis [16–18]. Densitometric analysis performed in the absence of saturation for CaM mutants as compared to CaM^{WT} and revealed that RyR2 binding to all CaM mutant proteins (CaM^{N98I}, CaM^{D132E}, CaM^{D134H} and CaM^{Q136P}) was significantly decreased compared to CaM^{WT} in the presence of Ca^{2+}. In contrast, in the absence of Ca^{2+}, statistically significant reduction on CaM-RyR2 binding was only observed for the CaM^{D134H} mutant (Fig. 3). Our co-IP data suggest that while the effect of D134H mutation on RyR/CaM association appears to be Ca^{2+}-independent, the N98I, D132E and Q136P mutations alter the interaction of CaM with RyR2 in a Ca^{2+}-dependent manner (Fig. 3).

To further investigate the potential effects of these cardiac disease-associated CaM mutations on RyR2 function and regulation, we performed a series of [^{3}H]ryanodine binding assays, as we have previously described [16–18]. The binding of [^{3}H]ryanodine to RyR is dependent upon the functional state of the channel and CaM has been shown to reduce the [^{3}H]ryanodine binding to RyR. The effect of CaM^{WT} and its corresponding mutants on [^{3}H]ryanodine binding to RyR2 was examined in a range of different Ca^{2+} concentrations varying from 10 nM to 100 μM. As shown in Fig. 4 and as anticipated, the CaM^{WT} significantly reduced the [^{3}H]ryanodine binding compared to the control (no addition of CaM protein). In contrast, none of the four CaM mutants was capable of inhibiting the [^{3}H]ryanodine binding to RyR2 at all high Ca^{2+} concentrations, as the level of [^{3}H]ryanodine binding was indistinguishable from that of the control, suggesting an impaired or no association of RyR2 with these CaM mutants.

Interestingly, in a previous study, where we characterized another CaM missense mutation at position 98, where asparagine (N) was replaced by a serine (S) residue, the CaM^{N98S} mutant displayed a similar RyR2-binding affinity to CaM^{WT}, and also in our [^{3}H]ryanodine binding assays CaM^{N98S} acted identically to CaM^{WT}, inhibiting RyR2 to the same extent [17]. In contrast, our current data reveals that the RyR2 binding of CaM^{N98I} was significantly decreased vs. CaM^{WT} at high Ca^{2+} concentrations, suggesting that the substitution of N by an S exerts a major inhibitory effect on the binding and regulation of CaM to RyR2 at high Ca^{2+} concentrations. This may be explained by the fact that residue N98 is directly involved in Ca^{2+} sequestration within EF hand 3 [20], and its replacement by an isoleucine (I) dramatically reduces the Ca^{2+}-binding affinity of CaM. This is supported by two independent studies that used a similar assay to measure the Ca^{2+}-binding affinities of N98S [7] and N98I [10] and showed that the N98S mutation results in a ~ 2 fold, while N98I in an ~8 fold decrease in the Ca^{2+}-binding affinities of CaM^{WT}. Moreover, crystallographic and NMR data for several arrhythmogenic CaM mutants reported by Wang et al., suggested that the N98I mutation causes a major distortion of CaM C-terminal lobe, resulting in a pathological conformation that alters its interaction with the IQ domain of the L-type voltage-gated Ca^{2+} channel ($Ca_v1.2$) [21]. In a similar fashion and based on the crystal structure, Wang et al., reported that when CaM^{Q136P} mutant is not bound to $Ca_v1.2$ IQ domain, it adopts a pathological conformation that can alter the interaction with other molecular targets, such as RyR2 [22]. Moreover, the clinical phenotypes of three patients bearing mutations at position N98 are very intriguing. Two patients with N98S or N98I mutations in CALM2 gene presented with LQTS phenotype [10], while one patient with N98S mutation in CALM1 had CPVT [7]. As mentioned earlier, in humans there are three CaM genes (*CALM1, CALM2 and CALM3*), which all encode an identical protein. The main difference is the relative expression of CaM in human cardiac tissue by the three genes, which was experimentally assessed and the ratio of CaM1:CaM2:CaM3 appeared to be approximately 1:2:5, respectively [8]. The identification of mutations such as the D132E and Q136P in patients with mixed LQTS and CPVT phenotypes [10] highlights the likelihood that specific clinical presentation(s) are triggered by multiple factors. These include the position of the mutation, the amino acid substitution, the ratio of mutant:WT protein, the total mutant protein concentration, or alterations on CaM Ca^{2+}-binding affinity, which in turn lead to defects in the vital interactions of CaM with

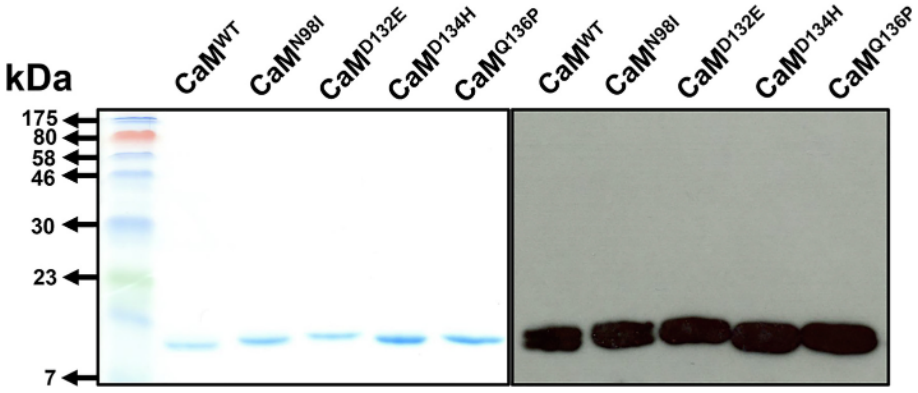

Fig. 2. Analysis of the purified recombinant CaM proteins. The affinity-purified CaM proteins (1 μg) were analyzed by 15% SDS-PAGE, followed by either Coomassie Brilliant Blue staining (left panel) or immunoblot analysis using an anti-CaM rabbit monoclonal antibody (1:10.000 dilution) (right panel). (For interpretation of the references to colour in this figure legend, the reader is referred to the web version of this article.)

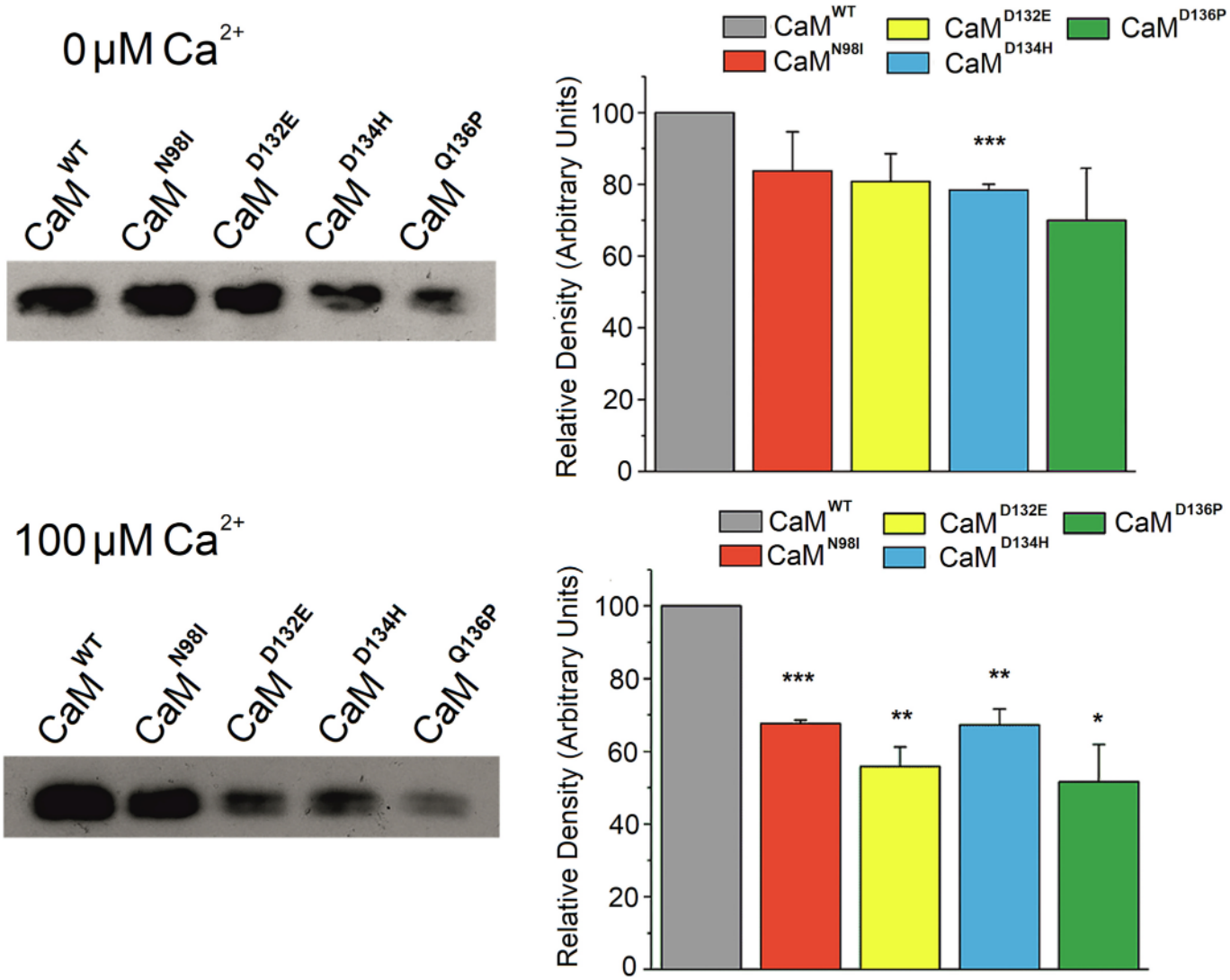

Fig. 3. Co-immunoprecipitation assays measuring the relative association of CaM^{WT} and CaM mutants with cardiac RyR2. RyR2 was immunoprecipitated with the anti-RyR2 Ab^{1093} from CHAPS-solubilised cardiac SR in the presence of 1 μM of exogenous recombinant CaM^{WT} or CaM mutant proteins, at two different Ca^{2+} concentrations (0 and 100 μM). The presence of RyR2-precipitated CaM^{WT} and CaM mutants was analyzed by 18% SDS-PAGE followed by immunoblot analysis using an anti-CaM rabbit monoclonal antibody (1:5000 dilution); (left panels). Following three independent experiments using three different porcine cardiac SR preparations, densitometry analysis (Quantity One® 1-D analysis software, BioRad) was performed for each occasion and the densities of the bands corresponding to CaM mutant proteins were normalized to CaM^{WT} (right panels). Differences in mean relative density between CaM^{WT} and CaM mutant proteins were compared using unpaired Student's *t*-test (GraphPad, Prism 5). Statistically significant differences are shown, * $P < 0.05$, ** $P < 0.005$ and ***$P < 0.001$ (All data are expressed as means ± SEM of 3 independent experiments, using three different porcine cardiac SR preparations with one technical repeat per SR preparation).

a plethora of ion channel complexes, including RyR2 [17].

Up to date, a number of linear fragments of RyR2 have been reported as potential CaM-binding sequences (CaMBDs), based on biochemical studies in which synthetic peptides or larger protein segments of RyR2 were used [4,23–25]. The sequence within the residues 3583-3603aa in RyR2, as well as extended versions of this sequence, which are highly conserved among mammalian RyR2 isoforms, have been identified as a CaM-binding site in almost all relevant studies and therefore this region is considered as a well-established CaMBD of RyR2 [14,23,25–28]. Deletion of the sequence 3583-3603aa in RyR2 resulted in disruption of CaM binding to RyR2 and reduced efficacy of CaM inhibition on RyR2 activity in single channel measurements [23]. Besides the 3583-3603aa region, other RyR2 regions have also been reported as potential CaM-binding sequences; however their exact contribution to CaM-binding remains to be fully elucidated [25,29]. Huang et al. [30], based on previous binding studies with radio-labeled CaM where sequence 4303–4328 in RyR1 (4261–4286 in RyR2) was first detected as a CaM-binding sequence [4,31], investigated the 3581-3612aa and 4261-4286aa regions of mouse RyR2 as putative CaMBDs by cryo-EM and FRET experiments. The above two RyR2-regions were found to be in close proximity and adjacent to the CaM-binding location, which was first localized on RyR2 by cryo-EM [32]. More specifically, these two sequences from the same subunit within the tetrameric RyR molecule have been reported to interact with each other, undergoing conformational changes when RyR2 switches between the closed and open states, forming an intra-subunit binding pocket for CaM [30]. These findings indicate the involvement of both the aforementioned RyR2-regions in RyR2-CaM binding. Moreover, Lau et al., [24] investigated the binding of CaM to three distinct regions of mouse RyR2, i.e. 1941-1965aa, 3580-3606aa and 4246-4276aa, by using ITC. The data obtained showed that all three RyR2-regions studied were bound to Ca^{2+}-CaM, while the C-terminal 4246-4276aa region of RyR2 exhibited the highest affinity among all for apo-CaM. In contrast, the region 1941-1965aa was shown to have significantly lower affinity compared to the other RyR2 CaM-

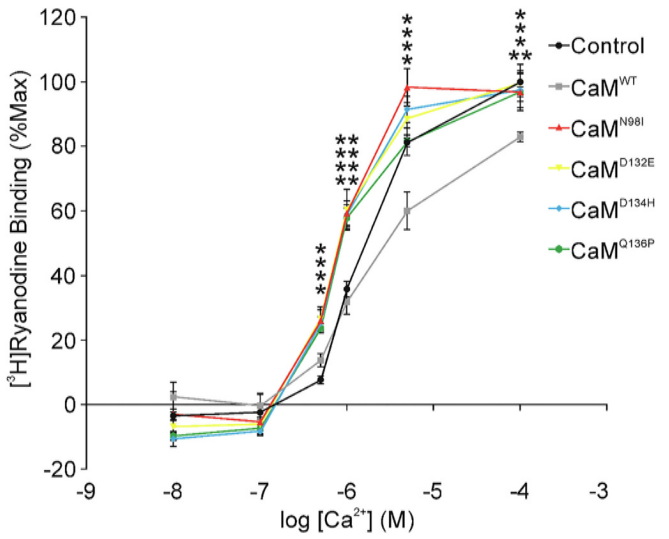

Fig. 4. [^{3}H]Ryanodine binding assays showing the impact of N98I, D132E, D134H and Q136P mutations on the ability of CaM to inhibit RyR2 open conformation. As described in the Materials and Methods section, the basic binding buffer contained 50 mM HEPES, 25 mM Tris, 500 mM KCl, pH 7.4 with either 1 mM EGTA (<0.01 μM Ca^{2+}) or with the indicated series of free Ca^{2+} concentrations. Normalized [^{3}H]ryanodine binding data are means ± SEM of 3 independent experiments. Unpaired Student's t-test (GraphPad, Prism 5) and statistically significant differences between control and CaM mutants are shown, * $P < 0.05$ and ** $P < 0.005$.

binding regions [24]. Furthermore, follow up studies from Brohus et al., [25] proposed a binding model where the C-domain of CaM is anchored to the well-established CaMBD (3581-3607aa) region of human RyR2 and saturated with Ca^{2+} during Ca^{2+}-oscillations, while the CaM N-domain functions as a dynamic Ca^{2+}-sensor that can bridge noncontiguous regions of RyR2 [25]. Interestingly, another recent crystallographic study revealed that binding of CaM to CaMBD3 (4246-4275aa) region and the binding of a fifth Ca^{2+} to CaM may contribute to the physiological regulation of RyR2 channel. It was demonstrated that the binding of the fifth Ca^{2+} to CaM results in a 2-fold increase in the binding affinity of CaM-CaMBD3 complex, which might be critical for the stabilization of the CaM-RyR2 complex under physiological conditions [33].

To investigate the interaction of CaM with this CaM-binding RyR2 region, we used recombinant CaM^{WT} protein and ITC experiments to screen a number of RyR2 specific synthetic peptides corresponding to the region 4240-4277aa of human RyR2. From all the synthetic peptides screened, we found one peptide, corresponding to region 4255-4271aa of human RyR2 (peptide F) that interacts with significant affinity to CaM in the presence and absence of Ca^{2+} (K_d values 0.60 and 16.58 μM, respectively); (Tables 1 and 2). Our findings regarding the binding of CaM to this RyR2 region is in good agreement with the previous Huang et al. study [30], suggesting that both 3584-3602aa and 4255-4271aa are critical for the interaction of RyR2 with CaM and might contribute to a mobile, intra-subunit CaM-binding domain. In order to examine how the N98I, D132E, D134H and Q136P mutations may alter the interaction of CaM with RyR2, we used ITC and we investigated the interaction of CaM^{WT} and its mutants with the two synthetic peptides, corresponding to the well-established CaMBD region 3584-3602aa (peptide B) and the region 4255-4271aa (peptide F). Fig. 5 shows typical ITC profiles at $T = 298.15$ K for the interactions between peptide B and CaM samples in holo-buffer. Negative power supply signals indicate exothermic interactions, while positive power supply signals correspond to endothermic events. Typically, large exothermic signals signify the formation of a network of favourable bonds between receptor and ligand, while endothermic events suggest that hydrophobic interactions are the driving force of the binding. All recombinant CaM proteins show significant affinity for peptide B, each forming a 1:1 complex with K_d values below 1 μM (Table 1). CaM^{D134H} and CaM^{Q136P} mutants appear to have a small negative effect on peptide B binding; in contrast to CaM^{N98I} and CaM^{D132E} that show higher affinity than CaM^{WT} (it is noteworthy that for CaM^{D132E}, the K_d is less than half of the WT's K_d). Peptide B binding is a strongly exothermic enthalpy-driven process, signifying an extensive network of interactions between the peptide and the protein.

In Fig. 6, the typical ITC profiles at $T = 298.15$ K for the interactions between peptide B and the five CaM proteins in apo-buffer are presented. From all recombinant CaM proteins tested, only CaM^{WT} was able to bind to peptide B with measurable affinity in the absence of Ca^{2+} (the lower K_d that can be detected with our ITC experimental protocol is 50 μM, so even if there is an interaction with lower affinity it will be biologically irrelevant), (Table 2). Contrary to holo-CaM, the apo-CaM-peptide B binding is a much weaker endothermic interaction ($K_{d\ (apo)} \sim 40{*}K_{d\ (holo)}$), with a complex formation that is based solely on entropically-favourable contributions. These entropically-favourable contributions generally arise by hydrophobic residues at the protein-solvent interface that are shielded from water upon binding. The ability of CaM to change conformations in response to intracellular Ca^{2+} levels leads to different peptide-protein interface geometries and thus different binding modes for the apo- and holo-CaM interactions. Our findings suggest that N98I, D132E, D134H and Q136P mutations prohibit apo-CaM from adopting a functional conformation.

Fig. 7 shows typical ITC profiles at $T = 298.15$ K for the interactions between peptide F and CaM samples in holo-buffer. All CaM proteins interact with peptide F, each forming a 1:1 complex, although mutated CaM proteins show significantly lower affinities for peptide F compared

Table 1
Thermodynamic parameters for the binding of peptides B (RyR2 3584-3602aa) and F (RyR2 4255-4271aa) with CaM wild type and mutants in holo-buffer. Dissociation constant [Kd], stoichiometry [N], binding enthalpy change [Δ_rH], entropic term change [$-T\bullet\Delta_rS$] and free energy change [Δ_rG] values obtained from titration of CaM^{WT} and CaM mutants with two appropriately selected synthetic peptides of human RyR2 (Peptide B and Peptide F). Titration was performed at $T = 298.15$ K in 100 mM KCl, 10 mM HEPES (pH 7.4), 10 mM $CaCl_2$. Values and corresponding errors were derived from non-linear least square fit of the ITC data to a one-set-of-sites thermodynamic model.

Titration		Dissociation Constant [K_d] (μM)	Stoichiometry [N]	Binding Enthalpy [Δ_rH] (kJ/mol)	Entropic Term [$-T\bullet\Delta_rS$] (kJ/mol)	Gibbs Free Energy Change [Δ_rG] (kJ/mol)
Peptide B	WT	0.35 ± 0.03	0.93 ± 0.01	−45.9 ± 1.4	9.1 ± 1.4	−36.8 ± 0.2
	N98I	0.29 ± 0.01	0.94 ± 0.01	−43.8 ± 1.3	6.5 ± 1.3	−37.3 ± 0.1
	D132H	0.16 ± 0.01	1.09 ± 0.01	−50.8 ± 1.6	11.9 ± 1.6	−38.9 ± 0.2
	D134H	0.36 ± 0.03	0.97 ± 0.01	−46.2 ± 1.5	9.5 ± 1.6	−36.7 ± 0.2
	Q136P	0.42 ± 0.02	0.97 ± 0.01	−47.9 ± 1.5	11.5 ± 1.6	−36.4 ± 0.1
Peptide F	WT	0.60 ± 0.05	1.05 ± 0.01	8.9 ± 0.4	−44.4 ± 0.5	−35.5 ± 0.2
	N98I	2.99 ± 0.28	1.04 ± 0.01	9.5 ± 0.4	−41.0 ± 0.5	−31.5 ± 0.3
	D132H	2.13 ± 0.15	1.06 ± 0.01	8.1 ± 0.4	−40.5 ± 0.5	−32.4 ± 0.2
	D134H	2.54 ± 0.39	1.16 ± 0.02	−10.9 ± 0.4	−21.1 ± 0.6	−31.9 ± 0.4
	Q136P	5.92 ± 0.50	1.09 ± 0.01	−10.5 ± 0.4	−19.3 ± 0.5	−29.8 ± 0.2

Table 2
Thermodynamic parameters for the binding of peptides B (RyR2 3584-3602aa) and F (RyR2 4255-4271aa) with CaM wild type and mutants in apo-buffer. Dissociation constant [K_d], stoichiometry [N], binding enthalpy change [Δ_rH], entropic term change [$-T\bullet\Delta_rS$] and free energy change [Δ_rG] values obtained from titration of CaM^{WT} and CaM mutants with two appropriately selected synthetic peptides of human RyR2 (Peptide B and Peptide F). Titration was performed at $T = 298.15$ K in 100 mM KCl, 10 mM HEPES (pH 7.4), 10 mM EDTA. Values and corresponding errors were derived from non-linear least square fit of the ITC data to a one-set-of-sites thermodynamic model.

Titration		Dissociation Constant [K_d] (μM)	Stoichiometry [N]	Binding Enthalpy [Δ_rH] (kJ/mol)	Entropic Term [$-T\bullet\Delta_rS$] (kJ/mol)	Gibbs Free Energy Change [Δ_rG] (kJ/mol)
Peptide B	WT	14.03 ± 2.40	1.04 ± 0.01	6.3 ± 0.9	−34.0 ± 1.0	−27.7 ± 0.4
	N98I	No binding detected				
	D132H	No binding detected				
	D134H	No binding detected				
	Q136P	No binding detected				
Peptide F	WT	16.58 ± 3.22	0.96 ± 0.01	6.6 ± 0.5	−33.9 ± 0.7	−27.3 ± 0.5
	N98I	No binding detected				
	D132H	No binding detected				
	D134H	No binding detected				
	Q136P	No binding detected				

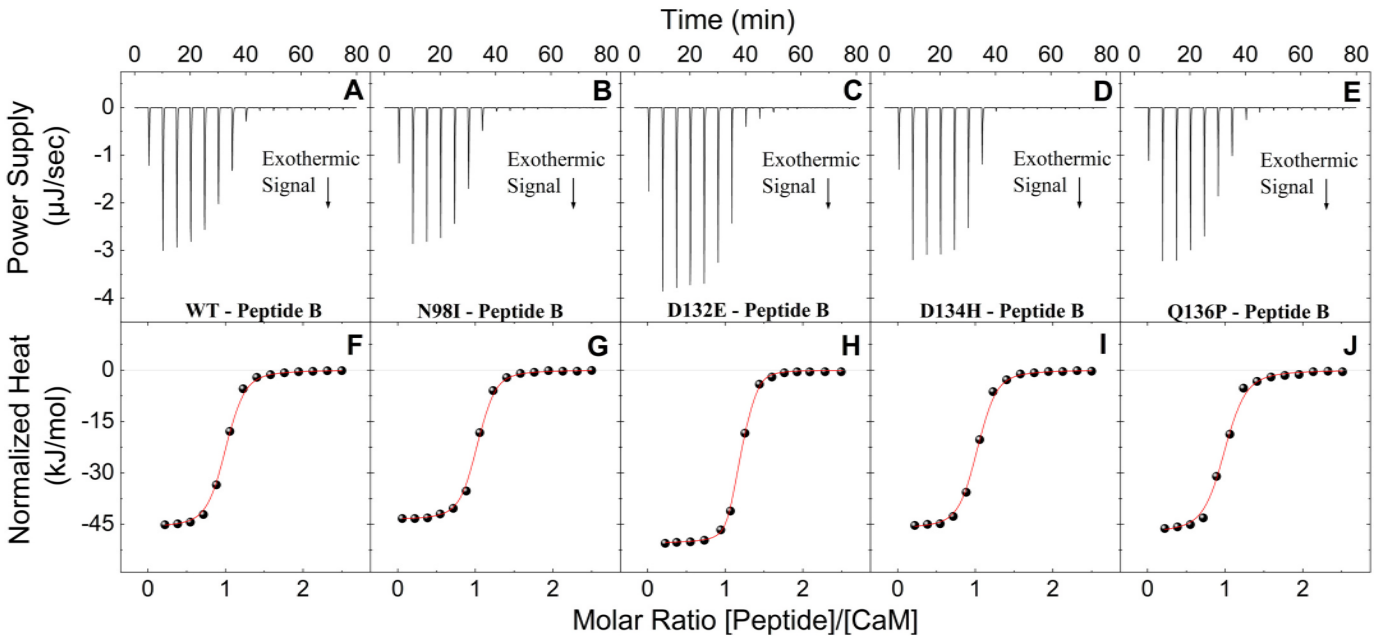

Fig. 5. Binding interactions of CaM wild-type and its corresponding mutants with peptide B (RyR2 3584-3602aa) in holo-buffer. Upper Panels: Change of power supply to the calorimetric cell during the titration of 450 μM of peptide B solutions into 40 μM of CaM^{WT} (A), CaM^{N98I} (B), CaM^{D132E} (C), CaM^{D134H} (D) and CaM^{Q136P} (E) at 298.15 K in holo-buffer, after the subtraction of the appropriate reference experiments. Lower Panels: Integration of the area under each injection, normalized per mol of injectant and plotted as a function of the [Peptide]/[CaM] ratio at each point of the CaM^{WT} (F), CaM^{N98I} (G), CaM^{D132E} (H), CaM^{D134H} (I) and CaM^{Q136P} (J) titrations. Solid red lines represent the non-linear least-square fit of the ITC data to a single-set-of-sites thermodynamic model. (For interpretation of the references to colour in this figure legend, the reader is referred to the web version of this article.)

to CaM^{WT} (~3–10 times lower, see Table 1). Interestingly, binding of CaM^{WT}, CaM^{N98I} and CaM^{D132E} to peptide F is endothermic, while the corresponding CaM^{D134H} and CaM^{Q136P} interactions are exothermic. This drastically different thermodynamic signature could suggest a different binding site or a different protein-peptide alignment for the CaM^{D134H} and CaM^{Q136P} - peptide F complexes.

In a similar fashion to CaM-Peptide B titrations, only CaM^{WT} was able to interact with peptide F in the absence of Ca^{2+} (Fig. 8). The apo-CaM interaction is ~30 times weaker compared to that of the holo-CaM, although it follows a similar entropically-driven process. The holo-CaM - peptide F binding has a more favourable entropic term that leads to this higher affinity. There are several possible mechanisms that could lead to that effect, like differences in complex flexibility and/or in the hydrophobic area shielded by the solvent. However, without supporting structural data this issue remains unclear. It is also interesting that apo-CaM^{WT} recognizes peptide F and peptide B with similar affinities (K_d = 16.58 and 14.03 μM, respectively).

Søndergaard et al. [34] recently reported the effect of various arrhythmogenic CaM mutations, including the four mutations that we investigated in this study, on the regulation of RyR2-mediated Ca^{2+} release during store-overload induced Ca^{2+} release (SOICR), as well as their effect on CaM-dependent inhibition of RyR2 Ca^{2+} release in permeabilized HEK293 cells [34]. The N98I, D132E and Q136P mutations affected the RyR2 activation threshold for SOICR suggesting that these mutations can promote spontaneous Ca^{2+} release in cardiomyocytes during diastole [27,34,35]. Furthermore, N98I, D132E, D134H and Q136P mutations impaired termination of RyR2 Ca^{2+} release suggesting that these arrhythmogenic CaM mutations can cause excessive Ca^{2+} release due to diminished inhibition of RyR2 during cardiomyocyte stimulation [34]. Moreover, the authors performed Ca^{2+}-dependent titration experiments of a fluorescently-labeled peptide corresponding to the CaMBD region 3581-3611aa of RyR2 with CaM and showed that the arrhythmogenic CaM mutations conferred a decreased affinity for binding to this peptide, altering the Ca^{2+}-dependency of CaM binding to

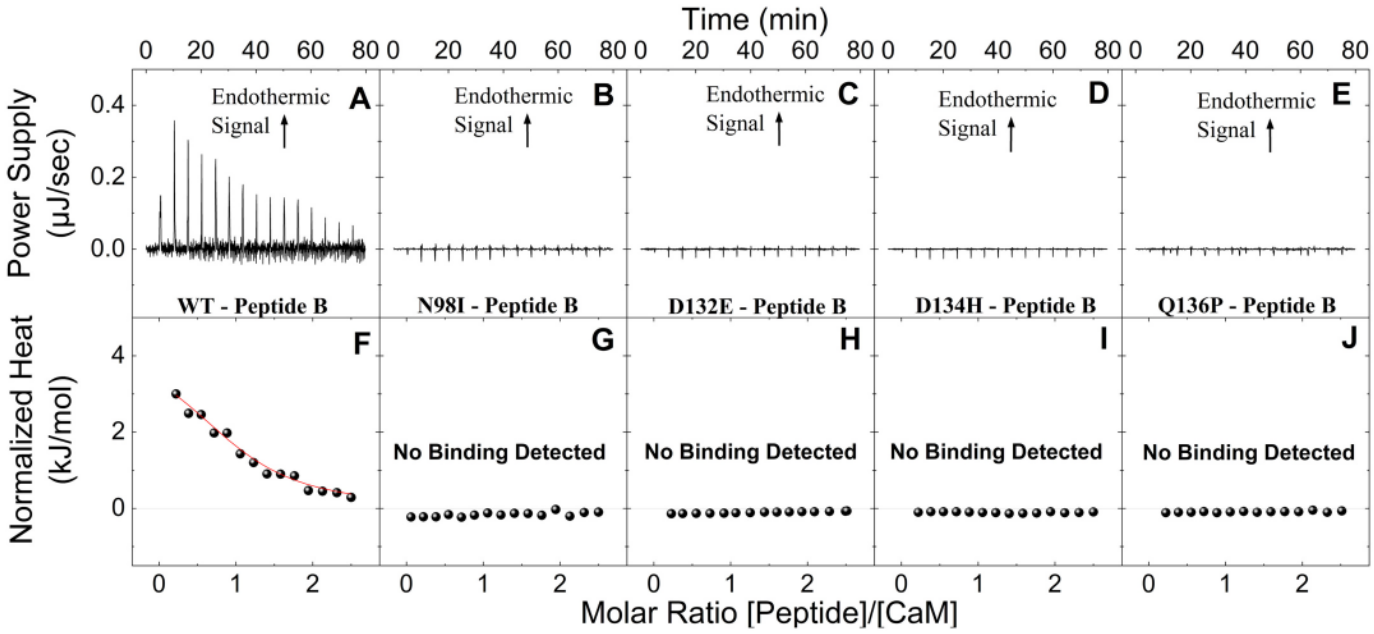

Fig. 6. Binding interactions of CaM wild-type and its corresponding mutants with peptide B (RyR2 3584-3602aa) in apo-buffer. Upper Panels: Change of power supply to the calorimetric cell during the titration of 450 μM of peptide B solutions into 40 μM of CaM^{WT} (A), CaM^{N98I} (B), CaM^{D132E} (C), CaM^{D134H} (D) and CaM^{Q136P} (E) at 298.15 K in apo-buffer, after the subtraction of the appropriate reference experiments. Lower Panels: Integration of the area under each injection, normalized per mol of injectant and plotted as a function of the [Peptide]/[CaM] ratio at each point of the CaM^{WT} (F), CaM^{N98I} (G), CaM^{D132E} (H), CaM^{D134H} (I) and CaM^{Q136P} (J) titrations. Solid red lines represent the non-linear least-square fit of the ITC data to a single-set-of-sites thermodynamic model. (For interpretation of the references to colour in this figure legend, the reader is referred to the web version of this article.)

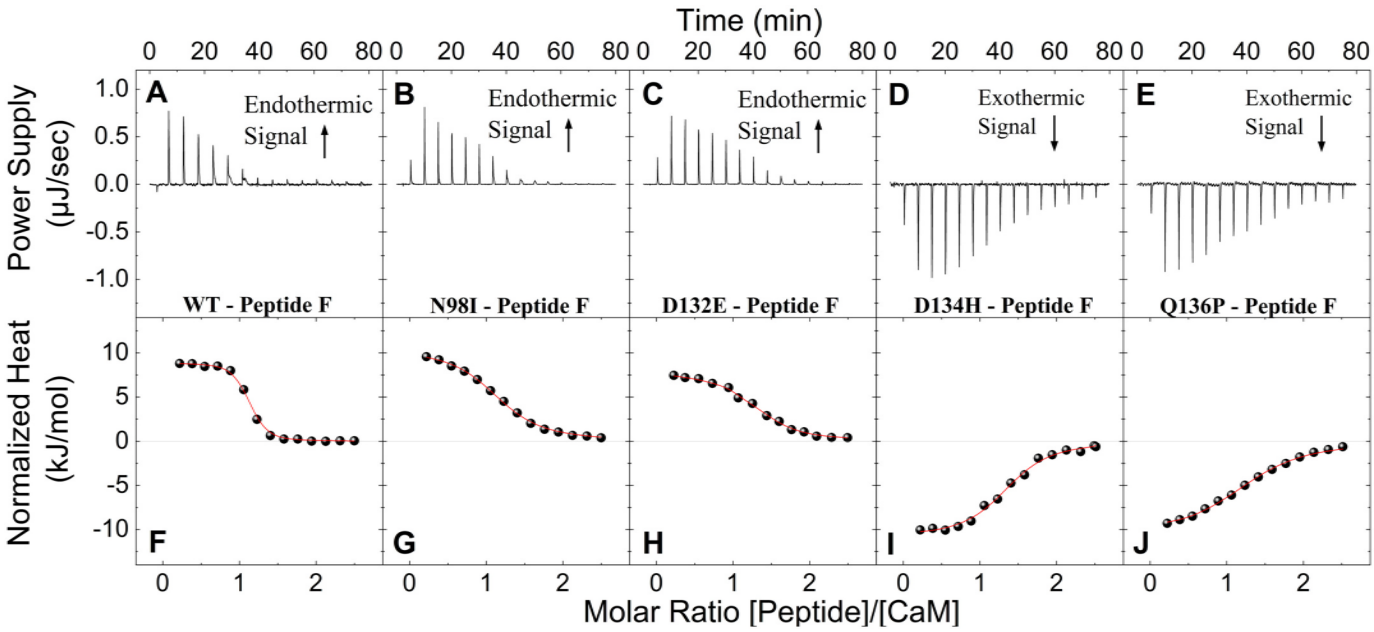

Fig. 7. Binding interactions of CaM wild-type and its corresponding mutants with peptide F (RyR2 4255-4271aa) in holo-buffer. Upper Panels: Change of power supply to the calorimetric cell during the titration of 450 μM of peptide F solutions into 40 μM of CaM^{WT} (A), CaM^{N98I} (B), CaM^{D132E} (C), CaM^{D134H} (D) and CaM^{Q136P} (E) at 298.15 K in holo-buffer, after the subtraction of the appropriate reference experiments. Lower Panels: Integration of the area under each injection, normalized per mol of injectant and plotted as a function of the [Peptide]/[CaM] ratio at each point of CaM^{WT} (F), CaM^{N98I} (G), CaM^{D132E} (H), CaM^{D134H} (I) and CaM^{Q136P} (J) titrations. Solid red lines represent the non-linear least-square fit of the ITC data to a single-set-of-sites thermodynamic model. (For interpretation of the references to colour in this figure legend, the reader is referred to the web version of this article.)

the RyR2 CaM-binding domain. Interestingly, the mutant CaM C-domains appeared to bind in a less Ca^{2+}-saturated state compared to the native CaM^{WT}/RyR2 CaMBD interaction at cardiomyocyte resting conditions and during early systole, supporting the authors proposal that a pathological defective CaM-RyR2 interaction can not only diminish RyR2 inhibition but can even facilitate RyR2 Ca^{2+} release [34].

On the other hand, the arrhythmogenic CaM N54I mutation which was previously identified in a patient with CPVT phenotype [7] and occurs in the loop between EF-hands 1 & 2 of the N-lobe domain has been shown to have no significant effect on the Ca^{2+} binding affinity of

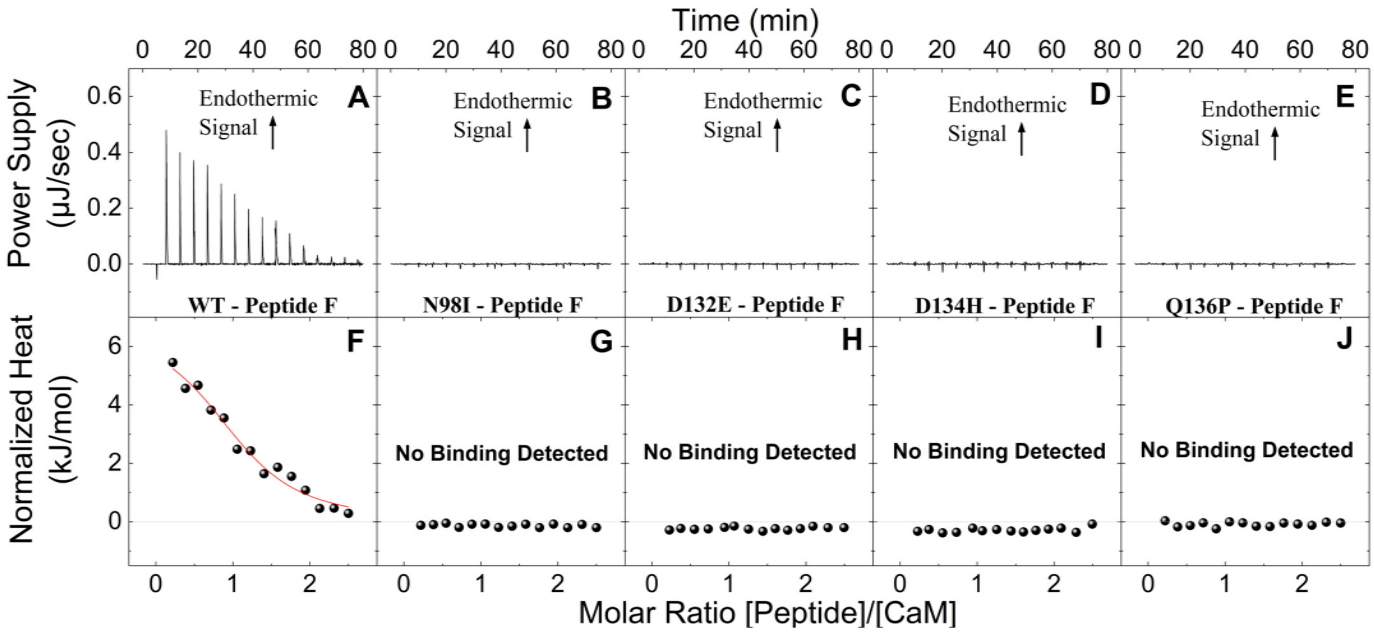

Fig. 8. Binding interactions of CaM wild-type and its corresponding mutants with peptide F (RyR2 4255-4271aa) in apo-buffer. Upper Panels: Change of power supply to the calorimetric cell during the titration of 450 μM of peptide F solutions into 40 μM of CaM^{WT} (A), CaM^{N98I} (B), CaM^{D132E} (C), CaM^{D134H} (D) and CaM^{Q136P} (E) at 298.15 K in apo-buffer, after the subtraction of the appropriate reference experiments. Lower Panels: Integration of the area under each injection, normalized per mol of injectant and plotted as a function of the [Peptide]/[CaM] ratio at each point of the CaM^{WT} (F), CaM^{N98I} (G), CaM^{D132E} (H), CaM^{D134H} (I) and CaM^{Q136P} (J) titrations. Solid red lines represent the non-linear least-square fit of the ITC data to a single-set-of-sites thermodynamic model. (For interpretation of the references to colour in this figure legend, the reader is referred to the web version of this article.)

CaM [17,36]. More importantly, this N-lobe CaM mutation showed an increased binding to RyR2 in ryanodine binding assays, which was not inhibitory but interestingly it enhanced RyR2 activity above that of the CaM-free control [17]. Moreover, in permeabilised ventricular myocytes, the N54I mutation showed to increase Ca^{2+} sparks and the frequency of Ca^{2+} waves [36]. Furthermore, the N54I mutation appeared to cause excessive RyR2 activity in HEK293 cells and in single RyR2 channels but showed to have no effect on the CaM C-domain/RyR2 CaMBD (3581-3607aa) interaction [34,36–38]. This raised the question of whether the CaM N-domain interacts with any other calmodulin binding region(s) of RyR2 rather than the 3581-3607aa, and that the N54I mutation impairs RyR2 inhibition by perturbing such interactions. Søndergaard et al. [38] assessed the effects of deleting each of the four known CaMBD regions in RyR2 on the CaM-dependent inhibition of RyR2-mediated Ca^{2+} release in HEK293 cells and found that only after deleting the RyR2-CaMBD 3581-3607aa could abolish the effects of both CaM-N54I and CaM-WT [38]. This supports the notion that CaM N54I mutation causes aberrant RyR2 regulation via an uncharacterized CaMBD or less likely CaMBD 3581-3607aa, and that likely CaMBD 3581-3607aa is required for the actions of both N- and C-domain CaM mutations [38].

In the present study, our ITC data suggest that both 3584-3602aa and 4255-4271aa RyR2 regions interact with significant affinity with wild-type CaM, in the presence and absence of Ca^{2+}. These two regions might contribute to a putative intra-subunit CaM-binding pocket, and the intracellular Ca^{2+} changes operate as an important "switch" for successful CaM/RyR2 association and thus channel regulation. In contrast, screening the interaction of the four arrhythmogenic CaM mutations (N98I, D132E, D134H and Q136P) with two synthetic peptides (B and F) that correspond to the aforementioned human RyR2 regions, revealed that all mutants show disparate binding properties to these two RyR2 peptides, in the presence and absence of Ca^{2+}. These findings indicate a more complicated picture suggesting differential mechanism(s) for CaM/RyR2 interaction and modulation of [^{3}H]ryanodine binding to RyR2. The resulting complexes seem to involve multiple RyR2 regions that cannot be recognized by these CaM mutants with high affinity. Further investigation is required to delineate the defective binding/interactions mechanisms between RyR2 and the pathogenic CaM mutants, as defective association of these two proteins is one of the main triggers of arrhythmogenesis and early onset sudden cardiac death.

Sources of funding

MN was supported by a QU Internal Grant "QUCG-CMED-19/20-2". The publication of this article was funded by Qatar National Library.

CRediT authorship contribution statement

Angelos Thanassoulas: Methodology, Formal analysis, Investigation, Data curation, Writing – review & editing. **Vyronia Vassilakopoulou:** Formal analysis, Investigation, Writing – review & editing. **Brian L. Calver:** Formal analysis, Investigation, Writing – review & editing. **Luke Buntwal:** Investigation. **Adrian Smith:** Investigation. **Christopher Lai:** Investigation. **Iris Kontogianni:** Investigation. **Evangelia Livaniou:** Methodology, Validation, Writing – review & editing, Supervision. **George Nounesis:** Methodology, Validation, Writing – review & editing, Supervision. **F. Anthony Lai:** Conceptualization, Methodology, Validation, Writing – review & editing, Supervision. **Michail Nomikos:** Conceptualization, Methodology, Validation, Investigation, Resources, Data curation, Writing – original draft, Writing – review & editing, Supervision.

Declaration of Competing Interest

None declared.

Data availability

Data will be made available on request.

Acknowledgments

We are grateful to Xuexun Fang (Laboratory of Molecular Enzymology and Enzyme Engineering of the Ministry of Education, Jilin University, China) for providing the pHSIE vector.

References

[1] F. Friedberg, A.R. Rhoads, Evolutionary aspects of calmodulin, IUBMB Life 51 (2001) 215–221.
[2] M.R. Tadross, I.E. Dick, D.T. Yue, Mechanism of local and global Ca2+ sensing by calmodulin in complex with a Ca2+ channel, Cell 133 (2008) 1228–1240.
[3] M.R. Beccia, S. Sauge-Merle, D. Lemaire, N. Bremond, R. Pardoux, S. Blangy, P. Guilbaud, C. Berthomieu, Thermodynamics of Calcium binding to the Calmodulin N-terminal domain to evaluate site-specific affinity constants and cooperativity, J. Biol. Inorg. Chem. 20 (2015) 905–919.
[4] D.M. Balshaw, L. Xu, N. Yamaguchi, D.A. Pasek, G. Meissner, Calmodulin binding and inhibition of cardiac muscle calcium release channel (ryanodine receptor), J. Biol. Chem. 276 (2001) 20144–20153.
[5] Y. Yang, T. Guo, T. Oda, A. Chakraborty, L. Chen, H. Uchinoumi, A.A. Knowlton, B. R. Fruen, R.L. Cornea, G. Meissner, D.M. Bers, Cardiac myocyte Z-line calmodulin is mainly RyR2-bound, and reduction is arrhythmogenic and occurs in heart failure, Circ. Res. 114 (2014) 295–306.
[6] R. Fischer, M. Koller, M. Flura, S. Mathews, M.A. Strehler-Page, J. Krebs, J. T. Penniston, E. Carafoli, E.E. Strehler, Multiple divergent mRNAs code for a single human calmodulin, J. Biol. Chem. 263 (1988) 17055–17062.
[7] M. Nyegaard, M.T. Overgaard, M.T. Sondergaard, M. Vranas, E.R. Behr, L. L. Hildebrandt, J. Lund, P.L. Hedley, A.J. Camm, G. Wettrell, I. Fosdal, M. Christiansen, A.D. Borglum, Mutations in calmodulin cause ventricular tachycardia and sudden cardiac death, Am. J. Hum. Genet. 91 (2012) 703–712.
[8] L. Crotti, C.N. Johnson, E. Graf, G.M. De Ferrari, B.F. Cuneo, M. Ovadia, J. Papagiannis, M.D. Feldkamp, S.G. Rathi, J.D. Kunic, M. Pedrazzini, T. Wieland, P. Lichtner, B.M. Beckmann, T. Clark, C. Shaffer, D.W. Benson, S. Kaab, T. Meitinger, T.M. Strom, W.J. Chazin, P.J. Schwartz, A.L. George Jr., Calmodulin mutations associated with recurrent cardiac arrest in infants, Circulation 127 (2013) 1009–1017.
[9] R.F. Marsman, J. Barc, L. Beekman, M. Alders, D. Dooijes, A. van den Wijngaard, I. Ratbi, A. Sefiani, Z.A. Bhuiyan, A.A. Wilde, C.R. Bezzina, A mutation in CALM1 encoding calmodulin in familial idiopathic ventricular fibrillation in childhood and adolescence, J. Am. Coll. Cardiol. 63 (2014) 259–266.
[10] N. Makita, N. Yagihara, L. Crotti, C.N. Johnson, B.M. Beckmann, M.S. Roh, D. Shigemizu, P. Lichtner, T. Ishikawa, T. Aiba, T. Homfray, E.R. Behr, D. Klug, I. Denjoy, E. Mastantuono, D. Theisen, T. Tsunoda, W. Satake, T. Toda, H. Nakagawa, Y. Tsuji, T. Tsuchiya, H. Yamamoto, Y. Miyamoto, N. Endo, A. Kimura, K. Ozaki, H. Motomura, K. Suda, T. Tanaka, P.J. Schwartz, T. Meitinger, S. Kaab, P. Guicheney, W. Shimizu, Z.A. Bhuiyan, H. Watanabe, W.J. Chazin, A. L. George Jr., Novel calmodulin mutations associated with congenital arrhythmia susceptibility, Circ. Cardiovasc. Genet. 7 (2014) 466–474.
[11] K. Takahashi, T. Ishikawa, N. Makita, K. Takefuta, T. Nabeshima, M. Nakayashiro, A novel de novo calmodulin mutation in a 6-year-old boy who experienced an aborted cardiac arrest, HeartRhythm Case Rep 3 (2017) 69–72.
[12] K. Kato, H.M. Isbell, V. Fressart, I. Denjoy, A. Debbiche, H. Itoh, J. Poinsot, A. L. George Jr., A. Coulombe, M.A. Shea, P. Guicheney, Novel CALM3 variant causing Calmodulinopathy with variable expressivity in a 4-generation family, Circ. Arrhythm. Electrophysiol. 15 (2022), e010572.
[13] N. Yamaguchi, N. Takahashi, L. Xu, O. Smithies, G. Meissner, Early cardiac hypertrophy in mice with impaired calmodulin regulation of cardiac muscle Ca release channel, J. Clin. Invest. 117 (2007) 1344–1353.
[14] J.J. Arnaiz-Cot, B.J. Damon, X.H. Zhang, L. Cleemann, N. Yamaguchi, G. Meissner, M. Morad, Cardiac calcium signalling pathologies associated with defective calmodulin regulation of type 2 ryanodine receptor, J. Physiol. 591 (2013) 4287–4299.
[15] X. Xu, M. Yano, H. Uchinoumi, A. Hino, T. Suetomi, M. Ono, H. Tateishi, T. Oda, S. Okuda, M. Doi, S. Kobayashi, T. Yamamoto, Y. Ikeda, N. Ikemoto, M. Matsuzaki, Defective calmodulin binding to the cardiac ryanodine receptor plays a key role in CPVT-associated channel dysfunction, Biochem. Biophys. Res. Commun. 394 (2010) 660–666.
[16] M. Nomikos, A. Thanassoulas, K. Beck, V. Vassilakopoulou, H. Hu, B.L. Calver, M. Theodoridou, J. Kashir, L. Blayney, E. Livaniou, P. Rizkallah, G. Nounesis, F. A. Lai, Altered RyR2 regulation by the calmodulin F90L mutation associated with idiopathic ventricular fibrillation and early sudden cardiac death, FEBS Lett. 588 (2014) 2898–2902.
[17] V. Vassilakopoulou, B.L. Calver, A. Thanassoulas, K. Beck, H. Hu, L. Buntwal, A. Smith, M. Theodoridou, J. Kashir, L. Blayney, E. Livaniou, G. Nounesis, F.A. Lai, M. Nomikos, Distinctive malfunctions of calmodulin mutations associated with heart RyR2-mediated arrhythmic disease, Biochim. Biophys. Acta 2015 (1850) 2168–2176.
[18] S.I. Da'as, A. Thanassoulas, B.L. Calver, K. Beck, R. Salem, A. Saleh, I. Kontogianni, A. Al-Maraghi, G.K. Nasrallah, B. Safieh-Garabedian, E. Toft, G. Nounesis, F.A. Lai, M. Nomikos, Arrhythmogenic calmodulin E105A mutation alters cardiac RyR2 regulation leading to cardiac dysfunction in zebrafish, Ann. N. Y. Acad. Sci. 1448 (2019) 19–29.
[19] C.E. Karachaliou, C. Liolios, C. Triantis, C. Zikos, P. Samara, O.E. Tsitsilonis, H. Kalbacher, W. Voelter, M. Papadopoulos, I. Pirmettis, E. Livaniou, Specific in vitro binding of a new (99m)Tc-radiolabeled derivative of the C-terminal decapeptide of prothymosin alpha on human neutrophils, Int. J. Pharm. 486 (2015) 1–12.
[20] R. Chattopadhyaya, W.E. Meador, A.R. Means, F.A. Quiocho, Calmodulin structure refined at 1.7 A resolution, J. Mol. Biol. 228 (1992) 1177–1192.
[21] K. Wang, C. Holt, J. Lu, M. Brohus, K.T. Larsen, M.T. Overgaard, R. Wimmer, F. Van Petegem, Arrhythmia mutations in calmodulin cause conformational changes that affect interactions with the cardiac voltage-gated calcium channel, Proc. Natl. Acad. Sci. U. S. A. 115 (2018) E10556–E10565.
[22] K. Wang, M. Brohus, C. Holt, M.T. Overgaard, R. Wimmer, F. Van Petegem, Arrhythmia mutations in calmodulin can disrupt cooperativity of ca(2+) binding and cause misfolding, J. Physiol. 598 (2020) 1169–1186.
[23] N. Yamaguchi, L. Xu, D.A. Pasek, K.E. Evans, G. Meissner, Molecular basis of calmodulin binding to cardiac muscle ca(2+) release channel (ryanodine receptor), J. Biol. Chem. 278 (2003) 23480–23486.
[24] K. Lau, M.M. Chan, F. Van Petegem, Lobe-specific calmodulin binding to different ryanodine receptor isoforms, Biochemistry 53 (2014) 932–946.
[25] M. Brohus, M.T. Sondergaard, S.R. Wayne Chen, F. van Petegem, M.T. Overgaard, Ca(2+)-dependent calmodulin binding to cardiac ryanodine receptor (RyR2) calmodulin-binding domains, Biochem. J. 476 (2019) 193–209.
[26] B.R. Fruen, D.J. Black, R.A. Bloomquist, J.M. Bardy, J.D. Johnson, C.F. Louis, E. M. Balog, Regulation of the RYR1 and RYR2 Ca2+ release channel isoforms by Ca2 +−insensitive mutants of calmodulin, Biochemistry 42 (2003) 2740–2747.
[27] M.T. Sondergaard, X. Tian, Y. Liu, R. Wang, W.J. Chazin, S.R. Chen, M. T. Overgaard, Arrhythmogenic calmodulin mutations affect the activation and termination of cardiac ryanodine receptor-mediated Ca2+ release, J. Biol. Chem. 290 (2015) 26151–26162.
[28] N. Yamaguchi, A. Chakraborty, T.Q. Huang, L. Xu, A.C. Gomez, D.A. Pasek, G. Meissner, Cardiac hypertrophy associated with impaired regulation of cardiac ryanodine receptor by calmodulin and S100A1, Am. J. Physiol. Heart Circ. Physiol. 305 (2013) H86–H94.
[29] D. Greene, M. Barton, T. Luchko, Y. Shiferaw, Computational analysis of binding interactions between the ryanodine receptor type 2 and calmodulin, J. Phys. Chem. B 125 (2021) 10720–10735.
[30] X. Huang, Y. Liu, R. Wang, X. Zhong, Y. Liu, A. Koop, S.R. Chen, T. Wagenknecht, Z. Liu, Two potential calmodulin-binding sequences in the ryanodine receptor contribute to a mobile, intra-subunit calmodulin-binding domain, J. Cell Sci. 126 (2013) 4527–4535.
[31] S.R. Chen, D.H. MacLennan, Identification of calmodulin-, Ca(2+)-, and ruthenium red-binding domains in the Ca2+ release channel (ryanodine receptor) of rabbit skeletal muscle sarcoplasmic reticulum, J. Biol. Chem. 269 (1994) 22698–22704.
[32] X. Huang, B. Fruen, D.T. Farrington, T. Wagenknecht, Z. Liu, Calmodulin-binding locations on the skeletal and cardiac ryanodine receptors, J. Biol. Chem. 287 (2012) 30328–30335.
[33] Q. Yu, D.E. Anderson, R. Kaur, A.J. Fisher, J.B. Ames, The crystal structure of calmodulin bound to the cardiac ryanodine receptor (RyR2) at residues Phe4246-Val4271 reveals a fifth calcium binding site, Biochemistry 60 (2021) 1088–1096.
[34] M.T. Sondergaard, Y. Liu, M. Brohus, W. Guo, A. Nani, C. Carvajal, M. Fill, M. T. Overgaard, S.R.W. Chen, Diminished inhibition and facilitated activation of RyR2-mediated Ca(2+) release is a common defect of arrhythmogenic calmodulin mutations, FEBS J. 286 (2019) 4554–4578.
[35] M.T. Sondergaard, Y. Liu, K.T. Larsen, A. Nani, X. Tian, C. Holt, R. Wang, R. Wimmer, F. Van Petegem, M. Fill, S.R. Chen, M.T. Overgaard, The Arrhythmogenic calmodulin p.Phe142Leu mutation impairs C-domain Ca2+ binding but not calmodulin-dependent inhibition of the cardiac ryanodine receptor, J. Biol. Chem. 292 (2017) 1385–1395.
[36] H.S. Hwang, F.R. Nitu, Y. Yang, K. Walweel, L. Pereira, C.N. Johnson, M. Faggioni, W.J. Chazin, D. Laver, A.L. George Jr., R.L. Cornea, D.M. Bers, B.C. Knollmann, Divergent regulation of ryanodine receptor 2 calcium release channels by arrhythmogenic human calmodulin missense mutants, Circ. Res. 114 (2014) 1114–1124.
[37] M.T. Sondergaard, A.B. Sorensen, L.L. Skov, K. Kjaer-Sorensen, M.C. Bauer, M. Nyegaard, S. Linse, C. Oxvig, M.T. Overgaard, Calmodulin mutations causing catecholaminergic polymorphic ventricular tachycardia confer opposing functional and biophysical molecular changes, FEBS J. 282 (2015) 803–816.
[38] M.T. Sondergaard, Y. Liu, W. Guo, J. Wei, R. Wang, M. Brohus, M.T. Overgaard, S. R.W. Chen, Role of cardiac ryanodine receptor calmodulin-binding domains in mediating the action of arrhythmogenic calmodulin N-domain mutation N54I, FEBS J. 287 (2020) 2256–2280.